Triple oxygen isotopic evidence for atmospheric nitrate and its application in source identification for river systems in the Qinghai-Tibetan Plateau

Xinghui Xia [a,*], Siling Li [a], Fan Wang [b], Sibo Zhang [a], Yunting Fang [c], Jianghanyang Li [d], Greg Michalski [d], Liwei Zhang [a]

[a] State Key Laboratory of Water Environment Simulation, School of Environment, Beijing Normal University, Beijing 100875, China
[b] Guangdong Province Key Laboratory for Climate Change and Natural Disaster Studies, School of Atmospheric Sciences, Sun Yat-sen University, Guangzhou 51027, China
[c] Institute of Applied Ecology, The Chinese Academy of Sciences, 72 Wenhua Road, Shenyang 110016, China
[d] Department of Earth and Atmospheric Sciences, Purdue University, 550 Stadium Mall, West Lafayette, IN 47907, USA

HIGHLIGHTS

- The average of $\Delta^{17}O_{atm}$ value of atmospheric nitrate in the QTP was 16.4‰.
- The $\Delta^{17}O_{atm}$ value in the QTP was lower than the low-elevation regions.
- The SIAR model was used to trace the contribution of riverine nitrate sources.
- Manure was one of the major sources to riverine nitrate in the QTP.
- Atmospheric precipitation accounted for 10%–19% of riverine nitrate in the QTP.

GRAPHICAL ABSTRACT
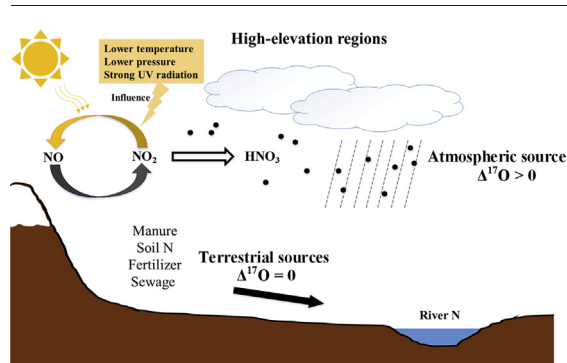
ABSTRACT

Nitrate source identification in river systems is important for water quality management. Recently, the oxygen isotopic anomaly of nitrate in atmospheric deposition ($\Delta^{17}O_{atm}$) is used to identify unprocessed atmospheric nitrate in river systems to reduce the uncertainty caused by the wide range of $\delta^{18}O$. In high-elevation regions, such as the Qinghai-Tibetan Plateau (QTP) featured with lower temperature and pressure as well as strong radiation, the $\Delta^{17}O_{atm}$ might be different from that in low-elevation regions, but no relevant studies have been reported. In this work, $\Delta^{17}O_{atm}$ in the QTP was studied, and the fingerprints of nitrate isotopes in synthetic fertilizer, livestock manure, domestic sewage, and soil organic nitrogen (SON) were identified and used to quantify various source contributions to riverine nitrate in the Yellow River and Changjiang River source regions located in the QTP during 2016–2017. The results showed that the average of $\Delta^{17}O_{atm}$ in the QTP was 16.4‰, lower than the range (19–30‰) reported for the low-elevation regions. The possible mechanism is decreased O_3 as well as increased hydroxyl and peroxy radical levels in the troposphere caused by the climate condition and ozone valley in the QTP will affect the production pathways of atmospheric nitrate. By combining the sewage discharge data with the output results of the SIAR (stable isotope analysis in R) model based on the stable isotope data, manure was determined to be one of the major sources to riverine nitrate for both rivers. The contributions of various sources to riverine nitrate were 47 ± 10% for manure, 30 ± 5% for SON, 10 ± 4% for atmospheric precipitation,

* Corresponding author.
  E-mail address: xiaxh@bnu.edu.cn (X. Xia).

$9 \pm 2\%$ for synthetic fertilizer, and $4 \pm 0\%$ for sewage in the Yellow River source region. This study indicates that the unique atmospheric conditions in the QTP have led to a lower $\Delta^{17}O_{atm}$ value, and atmospheric source makes a considerable contribution to riverine nitrate in the QTP.

1. Introduction

River systems play critical roles in global nitrogen cycle because rivers are important channels for nitrogen transport and complex "processors" for nitrogen transformation involving fixation, ammonium uptake, nitrification, denitrification, etc. (Rabalais, 2002; Mulholland et al., 2008; Xia et al., 2009; Liu et al., 2013b; Xia et al., 2017). During the past decades, extensive applications of synthetic fertilizer, discharge of municipal sewage, and burning of fossil fuels have contributed to high nitrogen loads in rivers, which results in acidification, eutrophication, deterioration of ecosystem, and increased human health risk (Kendall, 1998). Ambient nitrogen can enter rivers via atmospheric deposition, surface runoff, and diffusion (Alexander et al., 2007). To mitigate nitrogen loads in rivers and achieve sustainability of water resource utilization, we should identify nitrogen sources and then take rational strategies. By knowing sources and complex pathways for nitrogen into rivers, governors can make better policies for river management. The forms of nitrogen in rivers and streams include organic and inorganic nitrogen, and nitrate is the most thermodynamically stable form and it accounts for >80% of dissolved inorganic nitrogen (DIN) for most rivers in the world (Meybeck, 1982; Xia et al., 2002).

Stable isotope technique has been proven as a useful tool and applied widely to discriminate nitrate sources in aquatic systems. Different nitrate sources show unique $\delta^{15}N$ and $\delta^{18}O$ values; the $\delta^{15}N$ values of synthetic fertilizer range from −6‰ to +6‰, plant tissue from −5‰ to +2‰, manure from +5‰ to +25‰, sewage from +4‰ to +19‰, soil organic nitrogen (SON) from 0‰ to +9‰, and atmospheric N deposition from −15‰ to +15‰; the $\delta^{18}O$ values of atmospheric deposition range from +23‰ to +75‰, nitrate fertilizer from +17‰ to +25‰, and nitrate produced by nitrification from −10‰ to +15‰ (Kendall, 1998; Xue et al., 2009 and references therein). In the last decades, many studies have focused on the identification and quantification of nitrate inputs into water bodies with dual isotope method, and dominant contributor varies depending on the land use and hydrology of catchments (Ohte, 2013). However, the wide range of $\delta^{18}O$ in atmospheric nitrate and fractionation dynamics of biologic end member intrinsically restrict the application of $\delta^{18}O$ (Mayer et al., 2001). To overcome such limitation, recently there have been some studies on the application of $\Delta^{17}O$ to identify nitrate sources in river systems (Dejwakh et al., 2012; Liu et al., 2013a; Hale et al., 2014; Hundey et al., 2016). For majority of materials or processes on the earth, isotopic fractionation is mass-dependent and there is a common relationship between ^{18}O and ^{17}O isotope values expressed in delta notation as:

$$\delta^{17}O = 0.52 * \delta^{18}O \qquad (1)$$

However, unique mass-independent isotopic fractionation occurs during ozone (O_3) production, which makes the $\delta^{17}O$ value of O_3 significantly higher than the expected value based on $\delta^{18}O$ of O_3 (Thiemens, 1999). This is called "isotopic anomaly" and expressed as

$$\Delta^{17}O = \delta^{17}O - 0.52 * \delta^{18}O \qquad (2)$$

There is much evidence showing that the isotopic anomaly can be transferred from O_3 to other oxygen-bearing compounds during photochemical processes in the atmosphere (Fig. S1) (Thiemens, 1999; Michalski et al., 2003). Due to the participation of tropospheric ozone, atmospheric nitrate, formed via NO_x oxidation, will obtain a high $\Delta^{17}O$

value, and this $\Delta^{17}O$ value is not affected by mass-dependent biogeochemical processes such as denitrification or assimilation, which is helpful to distinguish atmospheric deposition from other pollution sources in rivers (Michalski et al., 2003; Michalski et al., 2004; Kendall et al., 2007).

In addition to O_3, many other species including trace gases (e.g. NO_x, VOCs) and radicals (e.g. OH, HO_2, RO_2) also participate in atmospheric nitrate production (Fig. S1), therefore the levels of these species and relevant environmental variables (e.g. temperature, pressure, solar radiation, relative humidity, and aerosol surface area) will also affect the $\Delta^{17}O$ value of atmospheric nitrate (denoted as $\Delta^{17}O_{atm}$). To date, there have been some model and field studies on transformation mechanisms, influencing factors, and spatiotemporal variability of $\Delta^{17}O_{atm}$ (Alexander et al., 2009; Morin et al., 2011; Shi et al., 2015; Guha et al., 2017). For example, a seasonal trend with lower $\Delta^{17}O_{atm}$ value during warmer months and higher value during colder months has been found in Canada, Eastern Asia, the USA, and coastal Antarctic (Michalski et al., 2003; Morin et al., 2007; Tsunogai et al., 2010). Besides, the $\Delta^{17}O_{atm}$ also shows significant spatial variations, the high-latitude regions such as Greenland, the Antarctic, and the Arctic, tend to have higher $\Delta^{17}O_{atm}$ values than the mid-latitudes (Patris et al., 2007; Kunasek et al., 2008; Morin et al., 2008; Michalski et al., 2012). The fluctuations of $\Delta^{17}O_{atm}$ over space and time are attributed to the changes of $\Delta^{17}O$ value in atmospheric O_3 (denoted as $\Delta^{17}O(O_3)$) and relative importance of O_3 during atmospheric nitrate production. As far as we know, there have been studies on the $\Delta^{17}O_{atm}$ values in polar areas and low-elevation areas at mid-latitudes. However, the $\Delta^{17}O_{atm}$ signatures have not been well constrained in high-elevation areas. Only Hundey et al. (2016) measured the $\Delta^{17}O$ value of snow samples in the Uinta Mountains (1281–3486 m a.s.l), and Guha et al. (2017) reported lower $\Delta^{17}O_{atm}$ values (5–15‰) in aerosol samples at Mt. Lulin (~3000 m).

As a typical high-elevation area, the Qinghai-Tibetan Plateau (QTP, >4000 m a.s.l) plays important roles in global geochemical cycle. It holds the headwaters of many large Asian rivers with the Yellow and Changjiang Rivers being two largest ones. The study on riverine nitrogen sources in the QTP will provide insight into nitrogen cycle for highland rivers. However, there has been no research on the riverine nitrogen source identification in the QTP. Moreover, the QTP is characterized with high elevation and strong solar radiation and photochemically active lower troposphere (Lin et al., 2008), suggesting that the atmospheric photochemical environment and processes in the QTP may differ from those of other areas in the same latitudes. Considering the mechanism of atmospheric nitrate production (Fig. S1), we expect that the climatic conditions in the QTP will affect production pathways of atmospheric nitrate. Low temperature and pressure in the QTP will lead to the variation of $\Delta^{17}O(O_3)$ according to the fitting equation ($\Delta^{17}O = 78.8P^{-0.122}$, $\Delta^{17}O = 16.2 + 0.06 \cdot T(K)$, Michalski et al., 2012). In addition, strong solar radiation in the QTP will affect the production of radicals such as peroxyl and hydroxyl radicals, further influencing the pathways of atmospheric nitrate production and consequently the $\Delta^{17}O_{atm}$ values. Yet, the $\Delta^{17}O_{atm}$ value in the QTP has not been reported. Thus, the adoption of the $\Delta^{17}O_{atm}$ values measured in other low-elevation areas might not be appropriate to estimate unprocessed atmospheric contribution to riverine nitrate in the QTP.

Therefore, we studied the stable isotopic composition of atmospheric nitrate in the QTP and subsequently applied it in the nitrate source identification for river systems in the source regions of the

Yellow River and Changjiang River located in the QTP. The main objectives were (1) to reveal the isotopic characteristics of atmospheric nitrate as well as the fingerprints of other sources including livestock manure, SON, sewage, and synthetic fertilizer in the QTP, (2) to investigate the temporal-spatial variations of riverine nitrate concentrations, and (3) to determine proportional contributions of various sources to riverine nitrate.

2. Materials and methods

2.1. The study area

The Yellow River source region (32°09′–36°33′ N, 95°53′–103°25′ E) (Li et al., 2018) and Changjiang River source region (32°26′–35°45′ N, 90°33′–95°20′ E) (Jiang et al., 2015) were taken as case studies (Fig. 1). The Yellow River source region, with a drainage area of 131,400 km^2 and mean elevation of >3000 m (a.s.l), represents 16.5% of the total area of the Yellow River basin. Affected by high elevation, the climate is characterized by strong UV and solar radiation (188–204 W/m^2), long sunshine duration (2400–2600 h per year), and low annual mean temperature (−4–1 °C) and humidity (53–60%) (Xu and He, 2006; You et al., 2010). The annual mean precipitation is about 530 mm, and about 75% of the total annual precipitation falls from June to September. The rainfall generally decreases from the southeast (800 mm) to the northwest (300 mm) (Zheng et al., 2007; Hu et al., 2012). The major vegetation is meadow, which accounts for 53.5% of the study area. Cultivated land accounts for only approximately 5.2% (Du et al., 2015), which is distributed mainly to the southeast of the Longyangxia reservoir, Guinan County. The Yellow River source region is underdeveloped without large industries, and sewage mainly consists of domestic wastewater. People mainly live in the flat terrain along river banks, and domestic wastewater is discharged directly into rivers due to lack of treatment facilities. Based on the difference of regional climatic conditions, land use types, and human activity intensity, the Yellow

River source region can be divided into three sections: MD–MT, MT–JG, and JG–LYX (Fig. 1); detailed information for each section can be found in Supporting Information.

The Changjiang River source region, with a drainage area of 137,800 km^2, represents 8.8% of the total area of the Changjiang River basin. Its climate, topography and vegetation conditions are similar to the Yellow River source region. Due to its higher elevation (>4000 m a.s.l), the annual mean temperature is below 0 °C and more glaciers and permafrost are distributed in this region compared to the Yellow River source region. Affected by such a harsh climate, the Changjiang River source region is sparsely populated (<2 km^{-2}). The local residents mainly settle in the downstream of the Tuotuohe station (Fig. 1) and they depend on livestock herding for a living.

2.2. Sampling and analysis

To trace nitrate sources, the rainwater samples were collected at four meteorological stations (Fig. 1 and Table S1) from April to October in 2016 during each precipitation event which occurred weekly or biweekly. The rainwater was collected with 5 L pre-cleaned pots and was split into 500 mL of clean plastic bottles within 12 h and transported to the laboratory as soon as possible. The precipitation amount for each event was measured with automatic rainfall gauges. In the laboratory, all samples were filtered with 0.2-μm polyethersulfone membranes and preserved at −20 °C until analysis. Diurnal variations of ambient temperature and rainfall in 2016 at each meteorological station are shown in Fig. S2. The rainfall from April to October contributed to approximately 94% of annual precipitation. Therefore, the average values of nitrate concentration and stable nitrate isotopes (δ^{15}N, δ^{18}O, and Δ^{17}O) during April to October can well represent their annual average values in rainwater. In addition, thirteen surface (0–10 cm) soil samples (Fig. 1) were collected during August in 2016, and grassland is the main vegetation type for the sampling sites. Six livestock manure samples (Fig. 1) were collected and two synthetic
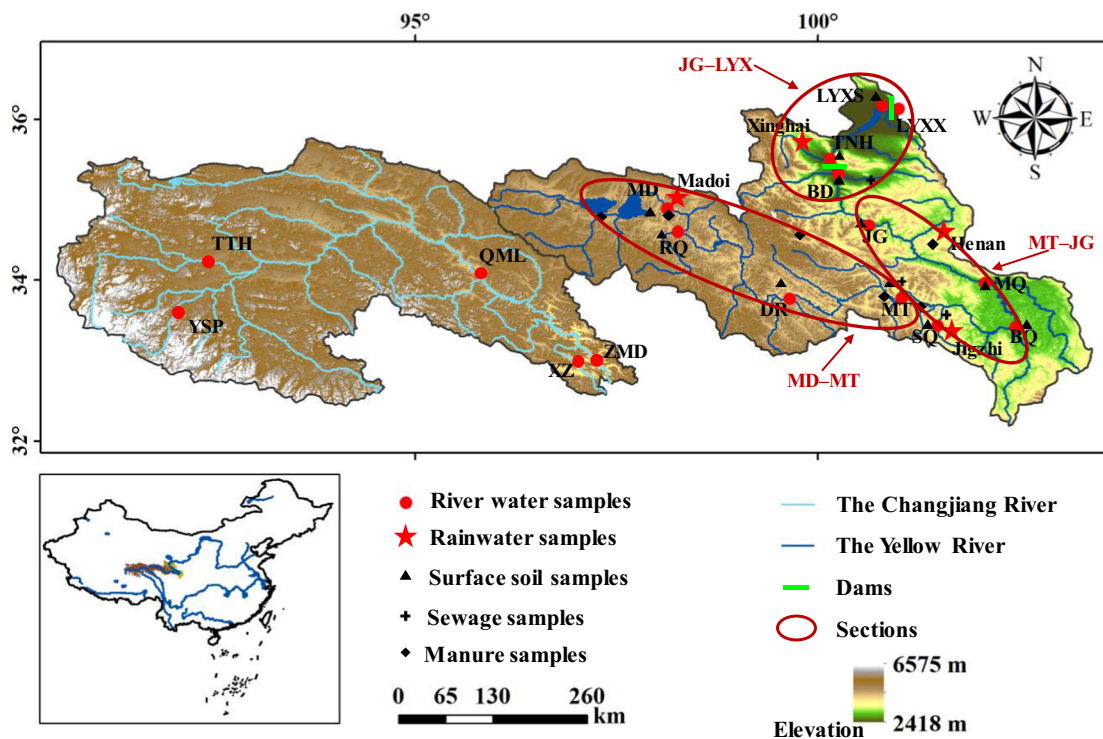
Fig. 1. The Yellow River and Changjiang River source regions showing the elevation and sampling sites. MD: Madoi; DR: Darlag; MT: Mentang; MQ: Maqu; JG: Jungong; BD: Banduo; TNH: Tangnag; LYXS: Upstream of the Longyangxia Dam; LYXX: Downstream of the Longyangxia Dam; RQ: Requ River; SQ: Shaqu River; BH: Baihe River. YSP: Yanshiping; TTH: Tuotuohe; QML: Qumalai; XZ: Xinzhai; ZMD: Zhimenda. The four meteorological stations for rainwater: Madoi, Jigzhi, Henan, and Xinghai.

fertilizer samples (urea and diammonium phosphate, SINOCHEM) were obtained from a local market. Three domestic sewage samples were collected from three major effluent ditches, respectively (Fig. 1). The river water samples were collected at 12 sites in the Yellow River source region during 5/30–6/15 (spring), 7/30–8/15 (summer), and 9/25–10/12 (autumn) in the non-frozen period of 2016, and 5 sites in the Changjiang River source region during 5/22–6/4 in 2017 (Fig. 1). The sampling sites were selected at hydrological stations except for the Longyangxia reservoir. In each sampling period, triplicate river water samples were collected at 20 cm-depth under the surface at each site and filtered with 0.2-μm polyethersulfone membranes on site within 24 h. All samples were preserved in a cooler and transported to the laboratory as soon as possible, after which the samples were stored in a freezer at −20 °C until analysis.

For the rainwater sample, the dissolved inorganic nitrogen (NO_3^-, NH_4^+, and NO_2^-) concentrations were determined by spectrophotometric method (Autoanalyser-3, Bran & Luebbe, France). The average nitrite concentration only accounted for 4.9% of the total concentration of nitrate and nitrite. The analysis of $\delta^{15}N$, $\delta^{18}O$, $\Delta^{17}O$ in nitrate was performed with a denitrifier method (Casciotti et al., 2002), by which nitrate was converted to N_2O and then decomposed into N_2 and O_2 in a heated gold tube (900 °C) for measurement via isotope ratio mass spectrometry (IRMS, Thermo Delta V). The obtained $\delta^{15}N$ and $\delta^{18}O$ values were respectively normalized to AIR and VSMOW (Standard Mean Ocean Water, oxygen) using the international reference materials (USGS-32, USGS-34, USGS-35, and IAEA-N-3). The analytic precisions (2σ) for $\delta^{15}N$, $\delta^{18}O$, $\Delta^{17}O$ were 0.4‰, 1.0‰, and 0.4‰, respectively, based on repeated measurements of the nitrate reference materials.

Because ammonium was the dominant nitrogen form in the sewage, manure, and fertilizer samples in this study and the soil samples mainly consisted of organic nitrogen, the $\delta^{15}N$ value of SON and $\delta^{15}N$-NH_4 of sewage, manure, and fertilizer were analyzed to represent the fingerprints of these potential riverine nitrate sources. The sewage samples were filtered with 0.2-μm polyethersulfone membranes, and the filtrate was collected. The manure samples were extracted with deionized water (m:v = 1:10) and filtered with 0.2-μm polyethersulfone membranes, and the filtrate was collected. Then NH_4^+ in the sewage and manure filtrate was extracted with diffusion method (Brooks et al., 1989) and $\delta^{15}N$-NH_4 was analyzed with EA-IRMS (ELEMENTAR-vario PYRO cube, ISOPRIME-100). The $\delta^{15}N$ of fertilizer samples was also determined with EA-IRMS. The soil samples were freeze-dried and ground to pass 100 meshes. After that, carbonate materials were removed with 0.5 M HCl and the soil samples were rinsed to neutral with deionized water. The solid residues were freeze-dried and analyzed with EA-IRMS for $\delta^{15}N$. The obtained $\delta^{15}N$ values were normalized to AIR using reference materials IAEA-N-1 and IAEA-N-3. The analytical precision (2σ) of $\delta^{15}N$ was 0.4‰. For the river water samples, the concentration and stable isotope ($\delta^{15}N$-NO_3, $\delta^{18}O$-NO_3, and $\Delta^{17}O$-NO_3) measurement of dissolved inorganic nitrogen were the same as the rainwater.

2.3. Mixing model

In this study, the SIAR model (stable isotope analysis in R, Parnell, 2008) was used to trace the contribution of nitrate sources. The SIAR model is a novel methodology for analyzing mixing models implemented in the R software package. The SIAR model combines Markov Chain Monte Carlo sampling with Bayesian updating to create posterior distributions of mixing fractions, which can be expressed as:

$$X_{ij} = \sum_{k=1}^{K} P_k \left(S_{jk} + c_{jk} \right) + \varepsilon_{ij} \tag{3-1}$$

$$S_{jk} \sim N\left(\mu_{jk}, \omega_{jk}^2\right) \tag{3-2}$$

$$c_{jk} \sim N\left(\lambda_{jk}, \tau_{jk}^2\right) \tag{3-3}$$

$$\varepsilon_{ij} \sim N\left(0, \sigma_j^2\right) \tag{3-4}$$

where X_{ij} is the value of isotope j ($j = 1, 2, 3, …, j$) of the mixture i ($i = 1, 2, 3, …, i$); P_k is the proportion of source k ($k = 1, 2, 3, …, K$), estimated by the model; S_{jk} is isotope j in source k, normally distributed with mean μ_{jk} and variance ω_{jk}^2. c_{jk} is the enrichment factor of isotope j in source k, normally distributed with mean λ_{jk} and variance τ_{jk}^2. ε_{ij} is the residual error, normally distributed with mean 0 and variance σ_j^2, and σ_j^2 is estimated by the model. By specifying the averages and standard deviations of source and mixture isotope fingerprints, the SIAR model allows users optionally input informative priors about the form of source contribution distributions, and the posterior probability distribution of the source contributions can be exported graphically and numerically. Different from the basic mass-balance linear mixing model (Xia et al., 2018), the SIAR model can incorporate a variety of sources of uncertainty including variability in isotope signatures and the lack of the unique solution in the case of many sources. Here, the SIAR model was applied to quantify the nitrate sources in the study area including nitrogen fertilizer, atmospheric precipitation, domestic sewage, and livestock manure.

3. Results

3.1. Inorganic nitrogen concentrations in atmospheric precipitation

The NO_3^- concentration in rainwater ranged from 4.3 to 117.9 μmol N/L (0.06–1.65 mg N/L) with a precipitation amount-weighted mean value of 15.0 μmol N/L (0.21 mg N/L), and NH_4^+ concentrations ranged from 6.4 to 77.1 μmol N/L (0.09–1.08 mg N/L) with a precipitation amount-weighted mean value of 26.4 μmol N/L (0.37 mg N/L), which were comparable to those in the Central Tibetan Plateau (Li et al., 2007) but lower than those in the Rocky Mountains (Wasiuta et al., 2015).

3.2. The stable isotopes of atmospheric nitrate and other potential nitrate sources

The $\delta^{15}N$ value of atmospheric nitrate in the Yellow River source region ranged from −10.2‰ to 16.4‰ with a precipitation amount-weighted mean value of −0.6‰; the $\delta^{18}O$ value of atmospheric nitrate ranged from 7.5‰ to 65.6‰ with a precipitation amount-weighted mean value of 35.0‰. The $\Delta^{17}O$ value of atmospheric nitrate ranged from 6.6‰ to 24.1‰ with a precipitation amount-weighted mean value of 16.4‰ (Table S2 and Fig. S3), and the arithmetic mean of $\Delta^{17}O_{atm}$ was 16.3 ± 3.9‰, which was used in the SIAR model under the assumption that the stable isotopic values of nitrate sources follow normal distribution (see Section 2.3). The nitrate stable isotope values in rainwater showed great spatiotemporal variation. For instance, most of $\delta^{15}N$ values were positive at the Madoi station in contrast to negative values at the other stations, and the observed $\delta^{18}O$ and $\Delta^{17}O$ values at the Madoi station were lower than those at the other stations. Active nitrogen in the atmosphere mainly comes from natural sources including soil emission, lightning, and biomass burning, and the spatiotemporal variation of these sources might lead to the great spatiotemporal variation of $\delta^{15}N$ values in the atmospheric deposition of this study. There were several extreme values in some rainwater samples (e.g. mid-September) which showed higher nitrate concentrations and lower $\delta^{18}O$ values, and it might be caused by the mixing of terrestrial nitrate in dust with nitrate in rainwater.

In addition to rainwater samples, SON, livestock manure, domestic sewage, and synthetic fertilizer samples were also collected to analyze terrestrial sources, and their isotopic fingerprints are shown in Table 1

Sources	$\delta^{15}N$ (‰)		$\Delta^{17}O$ (‰)	
	Range	Mean ± SD	Range	Mean ± SD
Fertilizer	−0.6–1.4	0.4 ± 1.0	−0.8–0.8	0 ± 0.8
Manure	10.2–20.2	13.6 ± 4.7	−0.8–0.8	0 ± 0.8
Sewage	4.7–10.6	6.2 ± 4.2	−0.8–0.8	0 ± 0.8
SON	3.8–7.9	5.6 ± 1.0	−0.8–0.8	0 ± 0.8
AP	−10.2–16.4	−0.6 ± 5.3	7.8–23.3	16.3 ± 3.9

and Fig. 2. The mean $\delta^{15}N$ values of various sources were 5.6 ± 1.0‰ for SON, 6.2 ± 4.2‰ for NH_4^+ of domestic sewage, 13.6 ± 4.7‰ for NH_4^+ of livestock manure, and 0.4 ± 1.0‰ for synthetic fertilizer. The $\delta^{15}N$ values of various sources were in the reported ranges summarized by Xue et al. (2009) and Xia et al. (2018). The $\delta^{15}N$ values of synthetic fertilizer and SON had smaller variability than other sources. This is because the nitrogen in ammonia fertilizer comes from the fixation of atmospheric N_2 (0‰) and little fractionation occurs in such process (Michalski et al., 2015). Soil is a great N pool and has a relatively steady $\delta^{15}N$ value (Kendall, 1998). The $\Delta^{17}O$ values of terrestrial sources should be zero theoretically due to mass-dependent fractionation, which were away from the atmospheric source. For the purpose of determining proportional contributions of riverine nitrate sources, the doubled value of analytic precision (−0.8‰ to 0.8‰) was used as a range of $\Delta^{17}O$ for terrestrial sources in the SIAR model (Table 1 and Fig. 2).

3.3. Nitrate concentrations and stable isotopes in river water

For the Yellow River source region, the NH_4^+ concentration of river water ranged from 1.3 to 11.2 μmol/L with a mean value of 5.0 μmol/L, and the NO_3^- concentration ranged from 0.5 to 51.2 μmol/L with a mean value of 28.2 μmol/L (Fig. 3), which accounted for 85% of the total dissolved inorganic nitrogen. The nitrate concentration increased along the mainstream during each sampling period in the Yellow
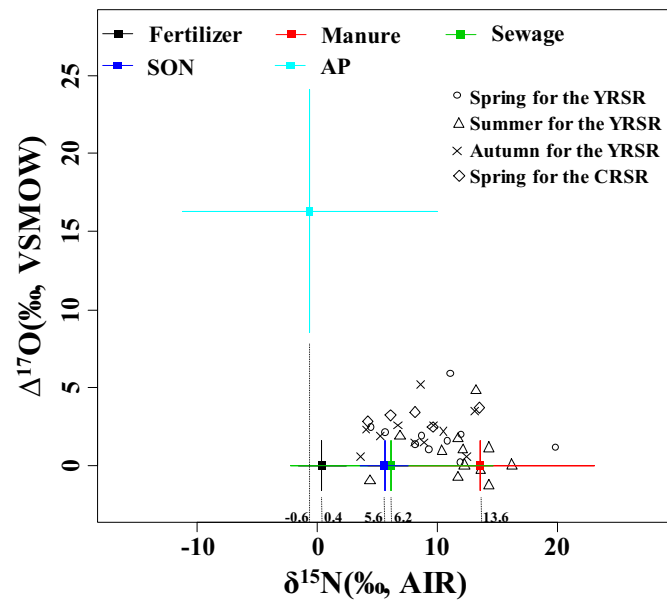
Fig. 3. Spatial and temporal variations of riverine DIN concentrations in the Yellow River source region.

River source region. It might be due to the increased and intensified nitrogen sources as well as the enhanced nitrification along the mainstream. The water temperature and dissolved oxygen demonstrated an increasing trend along the mainstream (Li et al., 2018), which provided more favorable conditions for microbial nitrification. In addition, there was no significant difference in DIN concentrations among different seasons for the Yellow River source region. The riverine nitrate concentration in the Changjiang River source region ranged from 32.2 to 50.1 μmol/L with a mean value of 43.7 μmol/L.

As shown in Fig. 2, the $\delta^{15}N$ value of riverine nitrate in the Yellow River source region ranged from 3.6‰ to 19.8‰ with a mean value of 10.1 ± 3.7‰. The $\delta^{18}O$ value ranged from −15.3‰ to 11.9‰ with a mean value of 0 ± 6.3‰, and the $\Delta^{17}O$ value ranged from −1.3‰ to 5.9‰ with a mean value of 1.6 ± 1.6‰, which were higher than the reported ranges for the lower-elevation areas of the Yellow River (Liu et al., 2013a, 2013b). The $\delta^{15}N$ value of riverine nitrate in the Changjiang River source region ranged from 4.2‰ to 13.5‰ with a mean value of 8.3‰; the $\delta^{18}O$ value ranged from 2.7‰ to 10.2‰ with a mean value of 6.0‰; the $\Delta^{17}O$ value ranged from 2.5‰ to 3.7‰ with a mean value of 3.1‰. The $\delta^{15}N$ values of most river water samples were distributed between those of manure and SON/sewage (Fig. 2), suggesting that these sources made major contributions to riverine nitrate. Considering both $\delta^{15}N$ and $\Delta^{17}O$ values, most river water samples fell between atmospheric and terrestrial sources, suggesting that atmospheric precipitation also contributed to riverine nitrate.

Fig. 2. $\Delta^{17}O$ versus $\delta^{15}N$ in river water samples and potential nitrate sources. The size of the error bar equals to the standard derivation mentioned in Table 1. SON: soil organic nitrogen; AP: atmospheric precipitation. The YRSR: the Yellow River source region; the CRSR: the Changjiang River source region.

3.4. Quantification of proportional contributions of various sources to riverine nitrate

As shown in Fig. S4, most of river water samples fell in the bottom left corner of the diagram with positive $\Delta^{17}O$ close to zero and low $\delta^{18}O$ values, while the rainwater samples had relatively high $\Delta^{17}O$ and $\delta^{18}O$ values. The $\delta^{18}O$ values of both rainwater and river water samples harbored wider ranges compared to $\Delta^{17}O$, therefore $\Delta^{17}O$ was more appropriate to identify atmospheric source of riverine nitrate. Consequently, the values of $\delta^{15}N$ and $\Delta^{17}O$ in combination with the SIAR model were used in this study to quantify the proportional contributions of various sources to riverine nitrate.

The output result of the SIAR model (Fig. S5 and Table S3) showed that the proportional contribution of sewage to riverine nitrate was almost equal to that of SON in the Yellow River source region in the three seasons; this result might be caused by that the sewage and SON had similar isotopic values. To distinguish the proportional contribution of these two sources, we used the output result of the SIAR model to estimate the sum of sewage and SON contribution. The N discharge from domestic wastewater (Table S4) was used to determine the contribution of sewage (detailed calculation is shown in Supporting Information), and the contribution of SON can be calculated by subtracting the contribution of sewage from the sum of sewage and SON.

As shown in Table 2, the average contributions of various sources to riverine nitrate in the Yellow River source region in the three seasons were 47 ± 10% for manure, 30 ± 5% for SON, 10 ± 4% for atmospheric precipitation, 9 ± 2% for synthetic fertilizer, and 4 ± 0% for sewage. The patterns of proportional contributions of various sources to riverine nitrate in the Yellow River source region were similar for different seasons, which were ordered by manure > SON > atmospheric precipitation ≈ fertilizer > sewage. Manure made the major contribution to riverine nitrate in each sampling period, which accounted for 42%, 62%, and 38% for spring, summer, and autumn, respectively (Table 2). The proportional contributions of atmospheric precipitation to riverine nitrate in the three seasons were 11% for spring, 4% for summer, and 13% for autumn.

As described in Section 2.1, there is little distribution of cropland in MD–MT and MT–JG sections of the Yellow River source region, therefore synthetic fertilizer was not taken into account for the two sections in the SIAR model. According to Table 2 and Fig. 4, proportional contributions of various sources to riverine nitrate in these two sections were ordered by manure > SON > atmospheric precipitation > sewage. Sewage and fertilizer could reflect human disturbance, and their total contributions to riverine nitrate were ordered by JG–LYX (15%) > MT–JG (6%) > MD–MT (3%), suggesting that anthropogenic interference increased with the distance from the headwater in the Yellow River source region. The contributions of atmospheric precipitation to riverine nitrate in various sections were shown as MT–JG (12%) > JG–LYX (8%) ≈ MD–MT (8%), which was consistent with the rainfall distribution that increased from the northwest to the southeast of the Yellow River source region.

In addition, to simplify the source identification process, the fingerprints of atmospheric precipitation, SON, sewage, and manure in the Changjiang River source region were assumed to be the same as those

in the Yellow River source region in view of the proximity of spatial locations and similarity of natural and social conditions between the two watersheds. Synthetic fertilizer was also not taken into account because there is almost no cropland in the Changjiang River source region. The proportional contributions of various sources to riverine nitrate were 47% for SON, 33% for manure, 19% for atmospheric precipitation, and 1% for sewage (Table 2 and Fig. 5). This result was comparable to that in the Yellow River source region.

4. Discussion

4.1. The flux of atmospheric nitrogen deposition

The average wet N deposition rate in the Yellow River source region could be estimated to be 3.3 kg N ha^{-1}y^{-1} based on the average inorganic nitrogen concentration of rainwater (0.62 mg N/L) and annual rainfall (530 mm). This rate was similar to contemporary N deposition for grassland around the world (2.81 kg N ha^{-1}y^{-1}, Holland et al., 1999), and comparable result was also documented in the Rocky Mountain (1.1 kg N ha^{-1}y^{-1}, Wasiuta et al., 2015) which is a high-elevation area in the same latitudes as the QTP. However, the estimated nitrogen deposition rate in the QTP was much lower than that of the North China Plain (27 kg N ha^{-1}y^{-1}, Zhang et al., 2008).

4.2. Nitrogen isotope variation of atmospheric nitrate

As shown in Table S2 and Fig. S3, the $\delta^{15}N$ values of atmospheric nitrate fell in the range of 15‰ -15‰ summarized by Xue et al. (2009) and Xia et al. (2018). Apart from the isotopic fractionation of N atom during the oxidation reaction of NO_x into NO_3^-, the variability of N isotopes could also be explained by the difference of N sources. Generally, if stationary sources (e.g. coal-fired power plants) control NO_3^- formation, the $\delta^{15}N$ value should be correlated with NO_x emission (Elliott et al., 2007). However, the $\delta^{15}N$ value of atmospheric nitrate in this study showed no significant correlation with nitrate concentration (Table S5) in spite of two large cities nearby, consequently, stationary source in large cities might not be the dominant factor. The negative correlation ($P < 0.05$, Table S5) of $\delta^{15}N$ value with ambient temperature was consistent with the results reported by Freyer et al. (1993) and Tsunogai et al. (2010); it could be due to the fact that lower temperature facilitated exchange reaction between NO and NO_2, which resulted in the enrichment of ^{15}N in produced nitrate (Kendall, 1998). It might interpret the phenomenon that most of $\delta^{15}N$ values were positive at the Madoi station with higher elevation and lower temperature, in contrast to negative values at the other stations with lower elevation and higher temperature (Table S2 and Fig. S2). However, this mechanism could not explain the difference in $\delta^{15}N$ values among other stations, which might be due to that other factors such as nitrate sources could also affect the $\delta^{15}N$ values. In addition, because of the lack of samples in colder months, whether this mechanism could work in winter needs further study.

4.3. Mechanism for the lower oxygen isotope values in atmospheric nitrate

Table S2 and Fig. S3 showed that the $\delta^{18}O$ values of atmospheric nitrate in the Yellow River source region fell in the reported range (25–75‰) around the world (Kendall et al., 2007; Xue et al., 2009), but lower than those (33.4–86.2‰) in South China (23°N) (Fang et al., 2011) and in Bermuda with the same latitude (32° N) as the study area (Hastings et al., 2003). The $\Delta^{17}O_{atm}$ values (mean 16.4‰) in the Yellow River source region were lower than the range (19–30‰) reported in previous studies for the low-elevation regions (Michalski et al., 2003; Michalski et al., 2004; Kendall et al., 2007; Savarino et al., 2008; Sofen et al., 2014; Nelson et al., 2018), and they were also lower than the reported values (mean 23.7‰, Hundey et al., 2016) for the Uinta Mountains with the elevation ranging from 1281 to 3486 m (a.s. l). Because the $\delta^{18}O$ and $\Delta^{17}O$ values in atmospheric nitrate are

Table 2
Proportional contributions of various sources to riverine nitrate in different sections and seasons. SON: soil organic nitrogen; AP: atmospheric precipitation.

Regions	Section/season	Manure	SON	AP	Fertilizer	Sewage
The Yellow River source region	MD–MT	57	32	8	–	3
	MT–JG	45	37	12	–	6
	JG–LYX	42	35	8	11	4
	Spring	42	32	11	10	5
	Summer	62	23	4	7	4
	Autumn	38	34	13	11	4
	Mean	47	30	10	9	4
The Changjiang River source region		33	47	19		1
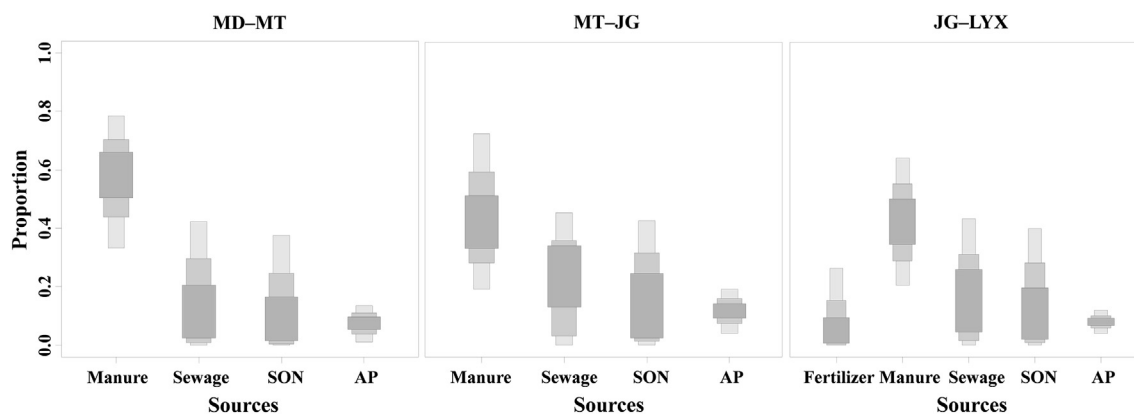
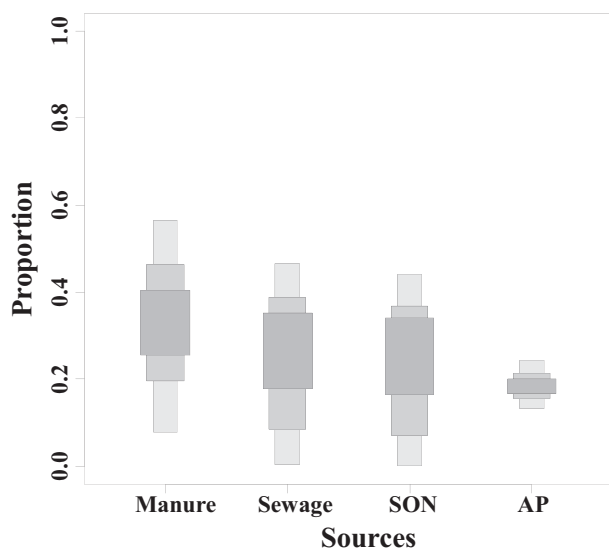**Fig. 4.** Probability distribution of proportional contributions of various sources to riverine nitrate in different sections in the Yellow River source region based on the SIAR model. The 50%, 75%, and 95% credible intervals are presented by the boxes from dark to light, respectively. The MD–MT section is featured with high elevation and alpine meadow; the MT–JG section is featured with grassland and small cities; the JG–LYX section is featured with cropland and denser population.

determined by the reactions that produce atmospheric nitrate (Hastings et al., 2003), the spatial variability of $\delta^{18}O$ and $\Delta^{17}O$ values in atmospheric nitrate and their difference between our study area and other sites can be explained by the production pathways of atmospheric nitrate.

As shown in Fig. S1, atmospheric nitrate is produced by NO_x oxidation via a series of pathways in which O atom plays a vital role. In the daytime, there is a rapid cycle between NO and NO_2 (Hastings et al., 2003; Morin et al., 2011; Shi et al., 2015):

$$NO + O_3 (or\ HO_2, RO_2, XO) \rightarrow NO_2 + O_2 \tag{R1}$$

$$NO_2 + O_2 \xrightarrow{h\nu} NO + O_3 \tag{R2}$$
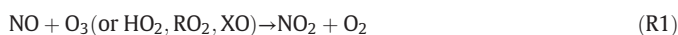
When sunlight is present, NO_2 is oxidized by hydroxyl radical (OH) into HNO_3:

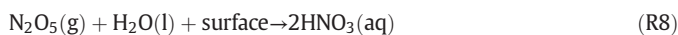$$NO_2 + OH + M \xrightarrow{h\nu} HNO_3 + O_2 \tag{R3}$$

Fig. 5. Probability distribution of proportional contributions of various sources to riverine nitrate in the Changjiang River source region based on the SIAR model. The 50%, 75%, and 95% credible intervals are presented by the boxes from dark to light, respectively.

NO_2 can also react with HO_2 into HNO_4, and HNO_4 will produce HNO_3 via hydrolysis reaction:

$$HNO_4 + H_2O \rightarrow HNO_3 + H_2O_2 \tag{R4}$$

At night and in colder environments, the oxidation reaction of NO_2 by O_3 is promoted and HNO_3 is produced via hydrogen abstraction by nitrate radical (NO_3) from dimethyl sulfide (DMS) or hydrocarbon (HC), and via heterogeneous hydrolysis of dinitrogen pentoxide (N_2O_5):

$$NO_2 + O_3 \rightarrow NO_3 + O_2 \tag{R5}$$

$$NO_3 + DMS\ or\ HC \rightarrow HNO_3 + products \tag{R6}$$

$$NO_2 + NO_3 + M \cdot \rightleftharpoons N_2O_5(g) + M \tag{R7}$$

$$N_2O_5(g) + H_2O(l) + surface \rightarrow 2HNO_3(aq) \tag{R8}$$

Similar to the diurnal variation mentioned above, the temperature and radiation fluctuations brought by seasonal variation can also alter the pathways of atmospheric nitrate production.

On the basis of the sources and life cycles of atmospheric NO_x mentioned above, oxygen atoms of atmospheric nitrate could come from oxygen (O_2), O_3, OH, and peroxy radical (HO_2/RO_2). It has been reported that the $\delta^{18}O$ mean value of troposphere O_2 is 23.5‰ (Kendall, 1998), and that of troposphere O_3 ranges from 90‰ to 120‰ (Johnston and Thiemens, 1997). The $\delta^{18}O$ range of OH is from −30‰ to 2‰ due to rapid oxygen isotope exchange with water vapor, while the oxygen atoms of peroxy radical actually come from atmospheric O_2 and their $\delta^{18}O$ values are close to O_2 in theory (Hastings et al., 2003; Fang et al., 2011). Therefore, higher $\delta^{18}O$ value of atmospheric nitrate reflects more participation of O_3, while lower value indicates more importance of hydroxyl and peroxy radicals. Except for O_3, the $\Delta^{17}O$ values of oxidants involving OH, RO_2, and HO_2 are near zero (Morin et al., 2011), thus non-zero $\Delta^{17}O_{atm}$ could be regarded as a result of O_3 participation in atmospheric NO_x oxidation reaction. The $\Delta^{17}O_{atm}$ value depends on $\Delta^{17}O(O_3)$, the oxidation parameters for NO and the mole fractions of different pathways (Michalski et al., 2012). This value would be relatively lower when OH pathway (R3) dominates atmospheric nitrate production, while it would be relatively higher when N_2O_5 pathway (R8) is dominant.

Considering the production mechanism of atmospheric nitrate, it could be inferred that the lower $\delta^{18}O$ and $\Delta^{17}O$ values of nitrate in rainwater observed in this study are related to the unique climate condition in the QTP. First, as mentioned in Sections 1 and 2.1, the QTP is characterized with high elevation, low pressure, and low temperature, which might affect the $\Delta^{17}O(O_3)$ value (Michalski et al., 2012). Second, Zhou

and Luo (1994) reported that an "ozone valley" occurred over the QTP in summer when the stratospheric ozone level was 10% lower than that over the East China Sea area in the same latitudes, which would increase the solar radiation reaching the troposphere and change atmospheric photochemical property in troposphere (Hansen et al., 1997), promoting the production of hydroxyl and peroxy radicals. Third, the main source of OH in troposphere is the reaction of water vapor with electronically excited O atom (^{1}D) produced by ozone photolysis in solar UV radiation (Chameides and Walker, 1973; Crutzen et al., 1999; Huang et al., 2009). The modeling result of Lin et al. (2008) showed that the mean concentration of OH was 3–8×10^6 cm^{-3} in the QTP, which was higher than that in free atmosphere at the same altitudes in lower-elevation areas, and also higher than the value (10.7×10^5 cm^{-3}) used for global $\Delta^{17}O_{atm}$ simulation in Alexander et al. (2009). Moreover, the level of tropospheric ozone was found lower in the QTP in all seasons, and especially in June, it was 40–50% lower than the surrounding areas (Huang et al., 2009). These facts suggested that atmospheric hydroxyl and peroxy radicals played more vital roles in atmospheric nitrate production compared to O_3, leading to the lower $\delta^{18}O$ and $\Delta^{17}O$ values in atmospheric nitrate in the QTP.

To further verify the influence of unique condition in the QTP on the $\Delta^{17}O_{atm}$, we calculated the $\Delta^{17}O_{atm}$ value based on photochemical steady-state approximation (Morin et al., 2011) as well as the background values of trace gases and radicals in the QTP (see Supporting Information), and the result showed that the estimated $\Delta^{17}O_{atm}$ value was 17–21‰, which was comparable to the mean value (15–20‰) in the QTP in summer (June-July-August) predicted by Alexander et al. (2009). The estimated $\Delta^{17}O_{atm}$ value in the QTP was close to the observed ones in the present study. Therefore, the lower $\delta^{18}O$ and $\Delta^{17}O$ values in atmospheric nitrate in the QTP can be interpreted as follows: the lower ambient temperature and pressure will affect $\Delta^{17}O$ value of ozone; the thin air and ozone valley in summer result in stronger radiation, and more UV rays can pass through the stratosphere; decreased O_3 as well as increased hydroxyl and peroxy radical levels in the troposphere ultimately contributes to lower $\delta^{18}O$ and $\Delta^{17}O$ values of rainwater. The slope of $\Delta^{17}O$ versus $\delta^{18}O$ plot can reflect the role of O_3 in making nitrate. As shown in Fig. S6, the slope is 0.20 (between 0 and 0.52), indicating the participation of O_3 is significant but not dominant. However, considering that the $\Delta^{17}O$ were lower than 15‰ in many samples at the Madoi station, this photochemical mechanism might not explain all variability. Another possible interpretation might be that eolian dust brought by westerly circulation (across desert and arid area) would result in the mix of nitrate from terrestrial sources with atmospheric nitrate, and the dilution effect would reduce the observed $\Delta^{17}O_{atm}$ value in wet deposition.

Similar to the present study, a lower $\Delta^{17}O_{atm}$ value has also been observed in some other studies. For example, a three-year observation of $\Delta^{17}O_{atm}$ in tropical (3° S) fog-water showed a range of 13–22‰ (Brothers et al., 2008). Alexander et al. (2009) used GEOS-Chem photochemical model to simulate global $\Delta^{17}O_{atm}$ value 0–200 m above the surface, and the result showed that the mean value of $\Delta^{17}O_{atm}$ around the world ranged from 7‰ to 41‰ with a lower value in the tropics. Moreover, lower $\Delta^{17}O_{atm}$ values (5–15‰) in aerosol samples were found in Taiwan (23° N) by Guha et al. (2017), and it was suggested that peroxy radical dominated the oxidation reaction of NO into NO_2, resulting in lower $\delta^{18}O$ and $\Delta^{17}O$ values of atmospheric nitrate. The unique climate condition in the QTP makes the photochemical process in the troposphere similar to that in the lower latitude, which might provide interpretation for the lower observed $\Delta^{17}O_{atm}$ value in the present study.

4.4. Comparison of riverine nitrate in the study area with other rivers

For both rivers in this study area, the riverine nitrate levels were higher than the average value (7 μmol/L) for unpolluted major world rivers (Meybeck, 1982; Turner et al., 2003). The finding suggests that

the riverine nitrogen load has been influenced by the growing human activities (Chen et al., 2014) in the Yellow River and Changjiang River source regions. However, the nitrate levels in the source regions were far lower than those in the middle and lower reaches of the Yellow River (309 μmol/L NO_3^-, Liu et al., 2013a) and Changjiang River (NO_3^- 60 μmol/L, Li et al., 2010), and this was because intensive urbanization and agricultural activities in the middle and lower reaches generated a large amount of pollution, while these human activities in the source regions were relatively lower because of sparser population density (2–16 km^{-2}, Table S4).

4.5. Relative importance of various sources

The Yellow River source region was taken here to assess the relative importance of various sources to riverine nitrate. The major source of riverine nitrate was manure (Table 2 and Fig. S5), which was due to the fact that a large amount of livestock was raised in this region. According to Gan and Hu (2016), manure from livestock in Qinghai Province was mainly produced by cattle (80%), followed by sheep (15%). In 2016, the number of livestock (cattle, sheep, and horse) was about 5.55×10^6 head in the Yellow River source region (Table S4), which accounted for 28.7% of that in Qinghai Province. On the basis of our calculation, the manure production from livestock in the Yellow River source region reached 25.5×10^6 t (Table S4). The grazing pattern in the QTP is rather extensive, therefore a large amount of manure produced by livestock is directly exposed to the environment without treatment. That means a large amount of immobile organic nitrogen fixed by plant is turned into mobile nitrogen via animals' digestion such as ammonium nitrogen. The nitrogen production from livestock manure was estimated to be 19.5×10^4 t N/year (Table S4), and this value might be increasing considering a trend of overgrazing (Dong et al., 2015) in this region, which was a huge potential nitrogen source for river systems.

The secondary source was SON. Soil erosion leads to great input of SON to rivers, and there are mainly three types of soil erosion: water erosion, freeze-thaw erosion, and wind erosion. With steep terrain and rugged topography, the Yellow River source region has a large drop gradient, which accelerates water erosion. In addition, freeze-thaw cycle generally occurs in cold or high-elevation regions because of huge diurnal temperature alteration, and this cycle increases mechanical denudation and thus chemical weathering (Li et al., 2018). Previous research (Zhang et al., 2007) showed that the freeze-thaw erosion was much extensive in the QTP, and freeze-thaw eroded area accounted for 55.3% of the Tibetan plateau. Furthermore, wind erosion caused by strong monsoon, vegetation degradation caused by overgrazing (Du et al., 2004), and climate warming (Yang et al., 2014) in the QTP also increase soil erosion, thus leading to the high contribution of SON to riverine nitrate.

The contribution of atmospheric precipitation to riverine nitrate for the Yellow River source region was relatively low compared to manure and sewage. According to the average nitrate concentration (0.21 mg N/L) in rainwater and annual rainfall (530 mm), the total amount of wet N deposition in the Yellow River source region could be estimated to be 1.3×10^4 t N/year, which was much lower than nitrogen production by livestock manure (Table S4). The contribution of atmospheric precipitation to riverine nitrate in the Yellow River source region was relatively higher than that in the middle and lower reaches of the Yellow River (Liu et al., 2013a). The comparison results suggested that the contribution of atmospheric source to riverine nitrate cannot be ignored in the study area. In addition, a little higher contribution of atmospheric source in the Changjiang River source region than that in the Yellow River source region might be due to a more intensified snowmelt event in this region during spring. This was also consistent with the result of the St. Lawrence River (Thibodeau et al., 2013), reflecting the importance of snowmelt events on riverine nitrate load.

The cultivated land accounts for only approximately 5% of the area in the Yellow River source region, and the fertilizer consumption was about 0.5×10^4 t N/year (Table S4), lower than that of the atmospheric N deposition. Thus, the contribution of synthetic fertilizer to riverine nitrate was not significant (9%). In addition, the proportional contributions of synthetic fertilizer and sewage in the Yellow River source region were lower than those in the middle and lower reaches of the Yellow River (Liu et al., 2013a).

4.6. Uncertainty analysis

Denitrification is one of the important nitrate sinks. When denitrification occurs, NO_3^- in water samples will enrich $\delta^{18}O$ and $\delta^{15}N$ with a statistical ratio of about 1:2 (Kendall, 1998), which has been applied in many studies involving surface water and groundwater systems (Dejwakh et al., 2012; Liu et al., 2013a; Lu et al., 2015). However, there was no significant linear correlation ($P > 0.05$, data not shown) between $\delta^{18}O$ and $\delta^{15}N$ of nitrate in river water, thus the isotopic fractionation resulting from denitrification process was not significant. Moreover, the application of $\Delta^{17}O$ avoided the interference of isotopic fractionation of $\delta^{17}O$ and $\delta^{18}O$ to source identification. Considering the spatial and seasonal variability of stable isotopic signatures in the mixture, the river water samples were divided into different groups, and the application of the SIAR model integrates some uncertainty including spatiotemporal variability of nitrate isotope values and the lack of deterministic solutions in case of many sources (Parnell et al., 2010).

However, there are some sources of uncertainty for attention. First, the $\delta^{15}N$ values of organic nitrogen in soil and ammonium in fertilizer, manure, and sewage were used in source identification of riverine nitrate, thus nitrification might result in unpredictable isotopic fractionation and introduce some uncertainty. According to previous studies (e.g. Kendall, 1998), mineralization usually causes a tiny fractionation ($\pm1\text{‰}$) between soil organic matter and soil ammonium. The estimation of fractionation associated with nitrification is very complex in natural systems. Such fractionation not only depends on environmental conditions but also on the size of the substrate pool, and the fractionation effect is weak when the substrate is almost consumed according to the Rayleigh equation. In this study, riverine nitrate was the major component of DIN, suggesting that fractionation caused by nitrification might not be significant. Moreover, the measured isotope values of fertilizer and soil N in the present study were comparable with the reported nitrified NH_4^+ fertilizer and soil N sources in other studies (Kendall, 1998; Xue et al., 2009). In some relevant studies (Korth et al., 2014; Kim et al., 2015; Hundey et al., 2016), the isotope values of SON and NH_4^+ in fertilizer were also used to trace nitrate sources in catchments. Second, due to the restriction of the sampling condition, the precipitation and river water samples during winter were not collected, which led to some uncertainty. Third, the calculation based on $\Delta^{17}O$ can only explain the part of unprocessed atmospheric nitrate entering rivers, but cannot explain the parts of processed nitrate and produced nitrate by atmospheric ammonium transformation in post-deposition process, which might underestimate the contribution of atmospheric source to riverine nitrate. Despite of above sources of uncertainty, the results in this study were consistent with the estimated nitrogen production of various sources as discussed in Section 4.5, which might provide insights for nitrogen management and pollution control in the Yellow River and Changjiang River source regions.

5. Conclusions

In this study, the $\Delta^{17}O$ value in atmospheric nitrate as well as the fingerprints of other sources were studied and used in source identification of riverine nitrate for the Yellow River and Changjiang River source regions located in the QTP. The observed $\delta^{18}O$ and $\Delta^{17}O$ values of atmospheric nitrate in this study were lower than those reported for low-elevation regions. This is because (1) lower ambient

temperature and pressure will affect $\Delta^{17}O$ value of ozone; (2) the thin air and ozone valley in the QTP in summer result in stronger radiation, and more UV ray can pass through the stratosphere; (3) the decreased O_3 concentration as well as increased hydroxyl and peroxy radical levels in the atmosphere alter the pathways of atmospheric nitrate production, and ultimately contribute to lower $\delta^{18}O$ and $\Delta^{17}O$ values of rainwater. Another possible interpretation might be the dilution effect caused by terrestrial nitrate in dust. In addition, the isotopic fingerprints of other sources including synthetic fertilizer, SON, manure, and sewage fell in the ranges of previous research.

The nitrate levels of river water for the Yellow River and Changjiang River source regions were higher than the average value for unpolluted major rivers in the world. The proportional contributions of various nitrate sources were ordered by manure > SON > atmospheric precipitation $\approx$ fertilizer > sewage for the Yellow River source region, and by SON > manure > atmospheric precipitation > sewage for the Changjiang River source region. Manure was one of the major sources to riverine nitrate; this might be due to that extensive livestock grazing pattern made a large amount of livestock manure directly exposed to the environment without treatment, resulting in a large quantity of mobile nitrogen entering rivers. It can be expected that the contribution of livestock manure would increase in the future considering a trend of overgrazing. The anthropogenic interference (sewage & synthetic fertilizer) increased with the distance from the headwater of the Yellow River source region, while the contribution of atmospheric precipitation to riverine nitrate in various sections was consistent with the spatial distribution of rainfall in the Yellow River source region. The contribution of atmospheric source in the studied area was higher than that in the middle and lower reaches of the Yellow River.

This study indicates that $\Delta^{17}O_{atm}$ will vary with atmospheric conditions, and atmospheric source makes a considerable contribution to riverine nitrate in the QTP. Livestock manure plays an important role in the riverine nitrogen load of the Yellow River and Changjiang River source regions. The results obtained at the present research would provide some guidance and reference for future nitrogen pollution control and water quality management in this water source conservation area.

Appendix A. Supplementary data

Supplementary data to this article can be found online at https://doi.org/10.1016/j.scitotenv.2019.06.204.

References

Alexander, R.B., Smith, R.A., Schwarz, G.E., Boyer, E.W., Nolan, J.V., Brakebill, J.W., 2007. Differences in phosphorus and nitrogen delivery to the Gulf of Mexico from the Mississippi River basin. Environmental Science & Technology 42, 822–830.

Alexander, B., Hastings, M., Allman, D., Dachs, J., Thornton, J., Kunasek, S., 2009. Quantifying atmospheric nitrate formation pathways based on a global model of the oxygen isotopic composition ($\Delta^{17}O$) of atmospheric nitrate. Atmos. Chem. Phys. 9, 5043–5056.

Brooks, P.D., Stark, J.M., McInteer, B.B., Preston, T., 1989. Diffusion method to prepare soil extracts for automated nitrogen-15 analysis. Soil Sci. Soc. Am. J. 53, 1707–1711.

Brothers, L.A., Dominguez, G., Fabian, P., Thiemens, M.H., 2008. Using multi-isotope tracer methods to understand the sources of nitrate in aerosols, fog and river water in Podocarpus National Forest, Ecuador. Agu Fall Meeting Abstracts.

Casciotti, K., Sigman, D., Hastings, M.G., Böhlke, J., Hilkert, A., 2002. Measurement of the oxygen isotopic composition of nitrate in seawater and freshwater using the denitrifier method. Anal. Chem. 74, 4905–4912.

Chameides, W., Walker, J.C.G., 1973. A photochemical theory of tropospheric ozone. J. Geophys. Res. 78, 8751–8760.

Chen, B., Zhang, X., Tao, J., Wu, J., Wang, J., Shi, P., Zhang, Y., Yu, C., 2014. The impact of climate change and anthropogenic activities on alpine grassland over the Qinghai-Tibet Plateau. Agric. For. Meteorol. 189, 11–18.

Crutzen, P.J., Lawrence, M.G., Pöschl, U., 1999. On the background photochemistry of tropospheric ozone. Tellus B: Chemical and Physical Meteorology 51, 123–146.

Dejwakh, N.R., Meixner, T., Michalski, G., McIntosh, J., 2012. Using ^{17}O to investigate nitrate sources and sinks in a semi-arid groundwater system. Environmental Science & Technology 46, 745–751.

Dong, Q.M., Zhao, X.Q., Wu, G.L., Chang, X.-F., 2015. Optimization yak grazing stocking rate in an alpine grassland of Qinghai-Tibetan Plateau, China. Environ. Earth Sci. 73, 2497–2503.

Du, M., Kawashima, S., Yonemura, S., Zhang, X., Chen, S., 2004. Mutual influence between human activities and climate change in the Tibetan Plateau during recent years. Glob. Planet. Chang. 41, 241–249.

Du, J., Shu, J., Xiong, S., 2015. Research on the Evaluation of Function of Water Reservation and Changes of Climate and Vegetation in the Yellow River Source Region. Science Press, Beijing (in Chinese).

Elliott, E.M., Kendall, C., Wankel, S.D., Burns, D.A., Boyer, E.W., Harlin, K., Bain, D.J., Butler, T.J., 2007. Nitrogen isotopes as indicators of NO_x source contributions to atmospheric nitrate deposition across the midwestern and northeastern United States. Environmental Science & Technology 41, 7661–7667.

Fang, Y., Koba, K., Wang, X., Wen, D., Li, J., Takebayashi, Y., Liu, X., Yoh, M., 2011. Anthropogenic imprints on nitrogen and oxygen isotopic composition of precipitation nitrate in a nitrogen-polluted city in southern China. Atmos. Chem. Phys. 11, 1313–1325.

Freyer, H.D., Kley, D., Volz-Thomas, A., Kobel, K., 1993. On the interaction of isotopic exchange processes with photochemical reactions in atmospheric oxides of nitrogen. Journal of Geophysical Research: Atmospheres 98, 14791–14796.

Gan, L., Hu, X., 2016. The pollutants from livestock and poultry farming in China—geographic distribution and drivers. Environ. Sci. Pollut. Res. 23, 8470–8483.

Guha, T., Lin, C.T., Bhattacharya, S.K., Mahajan, A.S., Ou-Yang, C.F., Lan, Y.P., Hsu, S.C., Liang, M.C., 2017. Isotopic ratios of nitrate in aerosol samples from Mt. Lulin, a high-altitude station in Central Taiwan. Atmos. Environ. 154, 53–69.

Hale, R.L., Turnbull, L., Earl, S., Grimm, N., Riha, K., Michalski, G., Lohse, K.A., Childers, D., 2014. Sources and transport of nitrogen in arid urban watersheds. Environmental Science & Technology 48, 6211–6219.

Hansen, J., Sato, M., Ruedy, R., 1997. Radiative forcing and climate response. J. Geophys. Res. 102, 6831–6864.

Hastings, M.G., Sigman, D.M., Lipschultz, F., 2003. Isotopic evidence for source changes of nitrate in rain at Bermuda. Journal of Geophysical Research: Atmospheres 108.

Holland, E.A., Dentener, F.J., Braswell, B.H., Sulzman, J.M., 1999. Contemporary and pre-industrial global reactive nitrogen budgets. Biogeochemistry 46, 7–43.

Hu, Y., Maskey, S., Uhlenbrook, S., 2012. Trends in temperature and rainfall extremes in the Yellow River source region, China. Clim. Chang. 110, 403–429.

Huang, F.X., Liu, N.Q., Zhao, M.X., 2009. Solar climatic signal of tropospheric ozone over the Tibetan Plateau. Chin. J. Geophys. 52, 913–921.

Hundey, E.J., Russell, S., Longstaffe, F., Moser, K.A., 2016. Agriculture causes nitrate fertilization of remote alpine lakes. Nat. Commun. 7.

Jiang, L., Yao, Z., Liu, Z., Wang, R., Wu, S., 2015. Hydrochemistry and its controlling factors of rivers in the source region of the Yangtze River on the Tibetan Plateau. J. Geochem. Explor. 155, 76–83.

Johnston, J.C., Thiemens, M.H., 1997. The isotopic composition of tropospheric ozone in three environments. Journal of Geophysical Research: Atmospheres 102, 25395–25404.

Kendall, C., 1998. Tracing nitrogen sources and cycling in catchments. In: Kendall, C., McDonnell, J.J. (Eds.), Isotope Tracers in Catchment Hydrogeology. Elsevier Science, Amsterdam, pp. 519–576.

Kendall, C., Elliott, E.M., Wankel, S.D., 2007. Tracing anthropogenic inputs of nitrogen to ecosystems. Stable Isotopes in Ecology and Environmental Science. 2, pp. 375–449.

Kim, K.H., Yun, S.T., Mayer, B., Lee, J.H., Kim, T.S., Kim, H.K., 2015. Quantification of nitrate sources in groundwater using hydrochemical and dual isotopic data combined with a Bayesian mixing model. Agric. Ecosyst. Environ. 199, 369–381.

Korth, F., Deutsch, B., Frey, C., Moros, C., Voss, M., 2014. Nitrate source identification in the Baltic sea using its isotopic ratios in combination with a Bayesian isotope mixing model. Biogeosciences 11, 4913–4924.

Kunasek, S.A., Alexander, B., Steig, E.J., Hastings, M.G., Gleason, D.J., Jarvis, J.C., 2008. Measurements and modeling of $\Delta^{17}O$ of nitrate in snowpits from Summit, Greenland. J. Geophys. Res. 113.

Li, C., Kang, S., Zhang, Q., Kaspari, S., 2007. Major ionic composition of precipitation in the Nam Co region, Central Tibetan Plateau. Atmos. Res. 85, 351–360.

Li, S.L., Liu, C.Q., Li, J., Liu, X., Chetelat, B., Wang, B., Wang, F., 2010. Assessment of the sources of nitrate in the Changjiang River, China using a nitrogen and oxygen isotopic approach. Environmental Science & Technology 44, 1573–1578.

Li, S., Xia, X., Zhou, B., Zhang, S., Zhang, L., Mou, X., 2018. Chemical balance of the Yellow River source region, the northeastern Qinghai-Tibetan Plateau: insights about critical zone reactivity. Appl. Geochem. 90, 1–12.

Lin, W., Zhu, T., Song, Y., Zou, H., Tang, M., Tang, X., Hu, J., 2008. Photolysis of surface O_3 and production potential of OH radicals in the atmosphere over the Tibetan Plateau. Journal of Geophysical Research: Atmospheres 113.

Liu, T., Wang, F., Michalski, G., Xia, X., Liu, S., 2013a. Using ^{15}N, ^{17}O, and ^{18}O to determine nitrate sources in the Yellow River, China. Environmental Science & Technology 47, 13412–13421.

Liu, T., Xia, X., Liu, S., Mou, X., Qiu, Y., 2013b. Acceleration of denitrification in turbid rivers due to denitrification occurring on suspended sediment in oxic waters. Environmental Science & Technology 47, 4053–4061.

Lu, L., Cheng, H., Pu, X., Liu, X., Cheng, Q., 2015. Nitrate behaviors and source apportionment in an aquatic system from a watershed with intensive agricultural activities. Environmental Science Processes & Impacts 17, 131.

Mayer, B., Bollwerk, S.M., Mansfeldt, T., Hütter, B., Veizer, J., 2001. The oxygen isotope composition of nitrate generated by nitrification in acid forest floors. Geochim. Cosmochim. Acta 65, 2743–2756.

Meybeck, M., 1982. Carbon, nitrogen, and phosphorus transport by world rivers. Am. J. Sci. 282, 401–450.

Michalski, G., Scott, Z., Kabiling, M., Thiemens, M.H., 2003. First measurements and modeling of $\Delta^{17}O$ in atmospheric nitrate. Geophys. Res. Lett. 30.

Michalski, G., Meixner, T., Fenn, M., Hernandez, L., Sirulnik, A., Allen, E., Thiemens, M., 2004. Tracing atmospheric nitrate deposition in a complex semiarid ecosystem using $\Delta^{17}O$. Environmental Science & Technology 38, 2175–2181.

Michalski, G., Bhattacharya, S.K., Mase, D., 2012. Oxygen isotope dynamics of atmospheric nitrate and its precursor molecules. Handbook of Environmental Isotope Geochemistry. Springer Berlin Heidelberg, pp. 613–635.

Michalski, G., Kolanowski, M., Riha, K.M., 2015. Oxygen and nitrogen isotopic composition of nitrate in commercial fertilizers, nitric acid, and reagent salts. Isotopes in Environmental & Health Studies 51, 382–391.

Morin, S., Savarino, J., Bekki, S., Gong, S., Bottenheim, J.W., 2007. Signature of Arctic surface ozone depletion events in the isotope anomaly ($\Delta^{17}O$) of atmospheric nitrate. Atmospheric Chemistry and Physics (ACP) & Discussions (ACPD).

Morin, S., Savarino, J., Frey, M.M., Yan, N., Bekki, S., Bottenheim, J.W., Martins, J.M., 2008. Tracing the origin and fate of NO_x in the Arctic atmosphere using stable isotopes in nitrate. Science 322, 730–732.

Morin, S., Sander, R., Savarino, J., 2011. Simulation of the diurnal variations of the oxygen isotope anomaly ($\Delta^{17}O$) of reactive atmospheric species. Atmos. Chem. Phys. 11, 3653–3671.

Mulholland, P.J., Helton, A.M., Poole, G.C., Hall, R.O., Hamilton, S.K., Peterson, B.J., Tank, J.L., Ashkenas, L.R., Cooper, L.W., Dahm, C.N., 2008. Stream denitrification across biomes and its response to anthropogenic nitrate loading. Nature 452, 202–205.

Nelson, D.M., Tsunogai, U., Ding, D., Ohyama, T., Komatsu, D.D., Nakagawa, F., Noguchi, I., Yamaguchi, T., 2018. Triple oxygen isotopes indicate urbanization affects sources of nitrate in wet and dry atmospheric deposition. Atmos. Chem. Phys. 18, 6381–6392.

Ohte, N., 2013. Tracing sources and pathways of dissolved nitrate in forest and river ecosystems using high-resolution isotopic techniques: a review. Ecol. Res. 28, 749–757.

Parnell, A., 2008. SIAR: Stable Isotope Analysis in R. http://cran.r-project.org/web/packages/siar/index.html.

Parnell, A.C., Inger, R., Bearhop, S., Jackson, A.L., 2010. Source partitioning using stable isotopes: coping with too much variation. PLoS One 5, e9672.

Patris, N., Cliff, S.S., Quinn, P.K., Kasem, M., Thiemens, M.H., 2007. Isotopic analysis of aerosol sulfate and nitrate during ITCT-2k2: determination of different formation pathways as a function of particle size. J. Geophys. Res. 112.

Rabalais, N.N., 2002. Nitrogen in aquatic ecosystems. AMBIO: A Journal of the Human Environment 31, 102–112.

Savarino, J., Bhattacharya, S.K., Morin, S., Baroni, M., Doussin, J.F., 2008. The $NO+O_3$ reaction: a triple oxygen isotope perspective on the reaction dynamics and atmospheric implications for the transfer of the ozone isotope anomaly. J. Chem. Phys. 128, 194303.

Shi, G., Buffen, A., Hastings, M., Li, C., Ma, H., Li, Y., Sun, B., An, C., Jiang, S., 2015. Investigation of post-depositional processing of nitrate in East Antarctic snow: isotopic constraints on photolytic loss, re-oxidation, and source inputs. Atmos. Chem. Phys. 15, 9435–9453.

Sofen, E., Alexander, B., Steig, E., Thiemens, M., Kunasek, S., Amos, H., Schauer, A., Hastings, M., Bautista, J., Jackson, T., 2014. WAIS Divide ice core suggests sustained changes in the atmospheric formation pathways of sulfate and nitrate since the 19th century in the extratropical Southern Hemisphere. Atmos. Chem. Phys. 14, 5749–5769.

Thibodeau, B., Hélie, J.-F., Lehmann, M.F., 2013. Variations of the nitrate isotopic composition in the St. Lawrence River caused by seasonal changes in atmospheric nitrogen inputs. Biogeochemistry 115, 287–298.

Thiemens, M.H., 1999. Mass-independent isotope effects in planetary atmospheres and the early solar system. Science 283, 341–345.

Tsunogai, U., Komatsu, D.D., Daita, S., Kazemi, G.A., Nakagawa, F., Noguchi, I., Zhang, J., 2010. Tracing the fate of atmospheric nitrate deposited onto a forest ecosystem in Eastern Asia using $\Delta^{17}O$. Atmos. Chem. Phys. 10, 1809–1820.

Turner, R.E., Rabalais, N.N., Justic, D., Dortch, Q., 2003. Global patterns of dissolved N, P and Si in large rivers. Biogeochemistry 64, 297–317.

Wasiuta, V., Lafrenière, M.J., Norman, A.-L., 2015. Atmospheric deposition of sulfur and inorganic nitrogen in the Southern Canadian Rocky Mountains from seasonal snowpacks and bulk summer precipitation. J. Hydrol. 523, 563–573.

Xia, X., Zhou, J., Yang, Z., 2002. Nitrogen contamination in the Yellow River basin of China. J. Environ. Qual. 31, 917–925.

Xia, X., Yang, Z., Zhang, X., 2009. Effect of suspended-sediment concentration on nitrification in river water: importance of suspended sediment-water interface. Environmental Science & Technology 43, 3681–3687.

Xia, X., Jia, Z., Liu, T., Zhang, S., Zhang, L., 2017. Coupled nitrification-denitrification caused by suspended sediment (SPS) in rivers: importance of SPS size and composition. Environmental Science & Technology 51, 212–221.

Xia, X., Zhang, S., Li, S., Zhang, L., Wang, G., Zhang, L., Wang, J., Li, Z., 2018. The cycle of nitrogen in river systems: sources, transformation, and flux. Environmental Science: Processes & Impacts 20, 863–891.

Xu, Z.X., He, W.L., 2006. Spatial and temporal characteristics and change trend of climatic elements in the headwater region of the Yellow River in recent 40 years. Plateau Meteorology 5, 018.

Xue, D., Botte, J., De Baets, B., Accoe, F., Nestler, A., Taylor, P., Van Cleemput, O., Berglund, M., Boeckx, P., 2009. Present limitations and future prospects of stable isotope methods for nitrate source identification in surface-and groundwater. Water Res. 43, 1159–1170.

Yang, K., Wu, H., Qin, J., Lin, C., Tang, W., Chen, Y., 2014. Recent climate changes over the Tibetan Plateau and their impacts on energy and water cycle: a review. Glob. Planet. Chang. 112, 79–91.

You, Q., Kang, S., Flügel, W.-A., Sanchez-Lorenzo, A., Yan, Y., Huang, J., Martin-Vide, J., 2010. From brightening to dimming in sunshine duration over the eastern and central Tibetan Plateau (1961–2005). Theor. Appl. Climatol. 101, 445–457.

Zhang, J., Liu, S., Yang, S., 2007. The classification and assessment of freeze-thaw erosion in Tibet. J. Geogr. Sci. 17, 165–174.

Zhang, Y., Liu, X.J., Fangmeier, A., Goulding, K.T.W., Zhang, F.S., 2008. Nitrogen inputs and isotopes in precipitation in the North China Plain. Atmos. Environ. 42, 1436–1448.

Zheng, H., Zhang, L., Liu, C., Shao, Q., Fukushima, Y., 2007. Changes in stream flow regime in headwater catchments of the Yellow River basin since the 1950s. Hydrol. Process. 21, 886–893.

Zhou, X., Luo, C., 1994. Ozone valley over Tibetan plateau. Journal of Meteorological Research 8, 505–550.